A Flexible Sierpinski Bow-tie Antenna for Search and Rescue Applications

[1]*Hidayath Mirza, [2]Nishat Sultana

[1]Department of Electrical and Electronic Engineering, College of Engineering and Computer Science, Jazan University, P.O. Box114, Jazan 45142, Saudi Arabia

[2]Department of Business Administration, Applied College, Jazan University, Jazan 45142, Kingdom of Saudi Arabia

Abstract - **The purpose of this research is to investigate the development of a low-profile flexible Sierpinski bow-tie antenna with fractal iterations. This antenna was constructed with the specific intention of meeting the requirements of search and rescue operations. During this examination, the antenna that is being shown here will act as the primary focus. The construction of a Flexible Sierpinski Bow-tie antenna, which is now under consideration, is going to take place on a substrate that is built of polydimethylsiloxane (PDMS) and has a relative permittivity of 2.7. Because of its desirable characteristics, such as its durability, flexibility, resistance to water, and adaptability for deployment in difficult environmental situations, PDMS was chosen as the system to be used. In order to make use of the search and rescue application, it is necessary to operate at a frequency of 406 MHz, which is a significantly lower frequency. This, in turn, requires the employment of antennas that have a longer electrical length. As a direct result of this, these antennas have a tendency to have bigger dimensions in terms of their physical dimensions. This assertion was validated by the findings of the simulation, which demonstrated that the antenna operated at a core frequency of 406 MHz and displayed a bandwidth of 65.53 MHz over its frequency range. As far as the antenna is concerned, the bandwidth is comparable to a fractional bandwidth percentage of 15.90% when the reflection coefficient is measured at a level of -10 dB.**

Keywords: wearable antennas; flexible antennas; compact antennas; search and rescue; Cospas-Sarsat.

I. INTRODUCTION

Aiming at bettering the identification and geolocation of distress signals in search and rescue (SAR) operations, the COSPAS-SARSAT system is a worldwide satellite-based radiolocation framework By means of a network of satellites and ground infrastructure to transfer vital data to rescue coordinating authorities, this worldwide program helps aviation, marine, and terrestrial users during emergencies. Two basic components define the architecture of the system:

COSPAS (an acronym from the Russian "Cosmicheskaya Systyema Poiska Aariynyich Sudov," meaning "Space System for the Search of Vessels in Distress") and SARSAT (Search and Rescue Satellite-Aided Tracking System), which taken together create a coherent network for the detection, processing, and reaction to emergency signals.

Driven by the need to improve search and rescue capacity for aviation and maritime crises, SARSAT was founded in the late 1970s through a joint effort involving France, Canada, and the United States. The Soviet Union built COSPAS as an auxiliary system concurrently. Recognizing the strategic benefits of interoperability, the four countries signed a cooperative agreement in 1979 under the International Civil Aviation Organization (ICAO) and the International Maritime Organization (IMO), so establishing the COSPAS-SARSAT program as a humanitarian project under their auspices. Supported by a hybrid satellite constellation of 62 active spacecraft spread throughout low-Earth orbit (LEOSAR), geostationary orbit (GEOSAR), and medium-Earth orbit (MEOSAR), the cooperation now consists of 45 member states. Operating at the internationally regulated frequency of 406 MHz, these satellites find and triangulate signals from Emergency Position-Indicating Radio Beacons (EPIRBs), Personal Locator Beacons (PLBs), and Emergency Locator Transmitters (ELTs).

The system uses Doppler shift methods to determine the distress position upon beacon activation, therefore obtaining an accuracy of roughly 2–5km for LEOSAR and producing almost immediate warnings with GEOSAR. Launched in 2018, MEOSAR satellites enhance accuracy to less than 100 meters by means of advanced GNSS (Global Navigation Satellite System) integration. After which Mission Control Centers (MCCs) deliver confirmed alerts to Rescue Coordination Centers (RCCs) in the affected area, distress signals are sent to Local User Terminals (LUTs) for decoding and validation. Usually taking ten to fifteen minutes, this thorough procedure helps SAR teams to be quickly deployed.

According to the COSPAS-SARSAT Secretariat, the system's efficiency is emphasized by its contribution to save

more than 54,000 lives since 1982. Its non-discriminatory approach provides easily available services for all countries, independent of their program participation. Standardized under the International Cospas-Sarsat Program Agreement, data-sharing protocols underline interoperability among member nations and support strict cybersecurity measures to prevent false alarms.

Recent advances include the addition of second-generation beacons with GNSS self-location capability and improved MEOSAR coverage, hence reducing latency and increasing dependability in polar and isolated environments. The system's architecture follows the United Nations' Global Maritime Distress and Safety System (GMDSS), therefore confirming its essential role as a basic component of worldwide humanitarian search and rescue operations. Current alliances with companies such as the European Galileo and U.S. GPS systems aim to improve coverage, so ensuring that the network fits the evolving technological and operational needs of the 21st century.[1]–[5].

Researchers from a wide range of academic institutions have presented research on the construction of antennas specifically for various functions, which has greatly advanced the field. These scientists have been delivering their results in the format of studies. Over the course of these studies, the crucial need of preserving the resilience of the antennas under demanding environmental conditions has been given thought. This has been achieved by using a broad spectrum of materials meant to stay in situ for a long period of time.In [6], An analysis has been carried out, and the focus of the investigation has been on the presentation of two distinct designs of meandering dipole antennas that operate at a frequency of 406 MHz. Among the two materials that are being evaluated for usage in the textile industry, one of the materials that is being considered is a non-conductive textile material. With a permittivity (ε_r) of 1.44 and a loss tangent ($\tan\delta$) of 0.044, the first textile material demonstrates its characteristics. A thickness of three millimeters can be found in it. Another sort of textile material is referred to as the shield, and it is the second type of textile material. In the design of the antennas that have been proposed, there are components that are conductive that are included. The conductivity of the layer is determined to be 1.18 x 105 S/m, while the thickness of the layer is measured to be 0.17 millimeters. The antenna being considered has a fractional bandwidth of 10.05%. The recommended antenna has dimensions of 200 x 75 x 3 mm3, which may alternatively be represented as $0.271\lambda_0 \times 0.102\lambda_0 \times 0.0041\lambda_0$. The antenna mentioned in reference [3] is a patch antenna of the type that functions at a frequency of 406 MHz [4], [7] . The conductive components of this product are manufactured through the use of an inkjet printing technique, while the substrate of this

product is constructed out of a foam substance that has a low loss. When the antenna is operating at a frequency of 406 MHz, its dimensions are specified as 283 x 65 x 17.5 mm^3, which is equivalent to $0.383\lambda_0 \times 0.088\lambda_0 \times 0.024\lambda_0$. The human body model was aligned in a parallel fashion with the antenna, and the distance between the antenna and the model was systematically altered between 0 and 200 millimeters to facilitate the experiment. It was decided to undertake an experiment in order to investigate the impact that water has on the return loss of an antenna. Changes were made to the gap distance between the antenna and the water, which ranged from 0 to 120 millimeters. This was accomplished. An innovative device that consists of two antennas and may be worn on a life vest was revealed by researchers in a study that was conducted not too long ago[8]. Another antenna is attached to the buoyant elements in the neck region, while the other antenna is connected to the buoyant components in the chest region. Both of these antennae are connected to the buoyant components. When it comes to the apparatus that is utilized in the process of saving lives, a standard breathing apparatus is utilized. The antenna is attached to the chest and neck regions of the buoyant component of the vest, and it contributes to the accomplishment of the goals that were intended for it. A Rohacell substrate was utilized in the creation of the antennas that were researched in this study. The antennas that were investigated were meandering dipole antennas that feature a folded configuration. The antennas exhibit resonance at a frequency of 406 MHz, which is the frequency at which such resonance occurs. In terms of dimensions, the antenna has dimensions of 300 × 150 × 1 mm^3, which may be expressed as $0.406\lambda_0 \times 0.203\lambda_0 \times 0.0014\lambda_0$. It also operates at a frequency of 406 MHz, which is another feature. The antenna that was proposed exhibits a fractional bandwidth that is comparable to 4% of the total bandwidth. The experiment resulted in a simulated increase of seven decibels while the antenna was positioned on the chest; however, when the antenna was relocated to the head position, the value experienced by the experiment decreased to one decibel. In the following article, a dual substrate antenna that can be utilized in search and rescue operations is presented. The antenna, which is a planar bow-tie antenna, comes with a Sierpinskifractal iterations as part of its functionality. With a resonance frequency of 406 MHz, the antenna that is being demonstrated has a maximum gain when it is positioned at an elevation of 0 degrees (pointing up at the sky). This is the position at which it gets the most power. The purpose of this work is to present potential alternatives to the kind of antennas that are already in use and that share these characteristics. The results of the simulation led to the conclusion that the antenna operated at a central frequency of 406 MHz and displayed a bandwidth of 228.8 MHz. This conclusion was reached based

on the findings of the simulation. It was demonstrated by the fact that the antenna worked at a fundamental frequency of 406 MHz, which was the operating frequency. This indicated that the antenna was functioning properly. The bandwidth in question is equivalent to a fractional bandwidth percentage, and it is equivalent to 58.8 percent of the total bandwidth when the reflection coefficient is assigned a value of -10 dB.

II. ANTENNA DESIGN

2.1 Materials

The building of the antenna that will be used for the purpose of the inquiry will involve the use of two materials that are distinct from one another. In the context of this discussion, the dielectric, which is represented by the symbol (ε_r), is utilized. The permittivity of the substrate ranges from 2.7 to 2.7. There is a copper clad coating that has a thickness of 0.035 millimeters and is utilized in both the radiating structure of the antenna as well as the reflective ground plane. The material has a thickness of 0.17 millimeters and an electrical conductivity of 1.18 x $⟦10⟧^5$ S/m which indicates that it is electrically conductive. For the purpose of this experiment, polydimethylsiloxane (PDMS) substrates are utilized. These substrates possess a permittivity (ε_r) of 2.7, a loss tangent (tanδ) of 0.02, and a thickness of 3 millimeters. Like those of SAR antennas, these properties are also present. In addition to polarizing converter surfaces, which have been demonstrated by Hidayath et al. and Hossain et al., ShieldIt Super and PDMS have both been utilized in the process of constructing antennas for satellite communications[9]–[11].

2.2 Physical Characteristics

Although it is simple to construct, the Sierpinski bow-tie antenna has the potential to become too big when operating at low frequencies. The construction of this antenna typically involves the use of suspended metal cut-outs or the use of a dielectric substrate as a primary support. In order to prevent the performance of the antenna from deteriorating, it is recommended that thin substrates with low permittivity be used whenever a substrate is utilized.

The antenna is made up of two Sierpinski gaskets that are stacked onto each other. The formation of a Sierpinski gasket begins with the formation of a metallic triangle that is analogous to one of the branches of a conventional bow tie. Removing the metallization from a triangle that was created by joining the center points of the initial triangle is the first step in the iteration process. In order to create the second iteration, the metallization of the mid-point triangles of the three metallized triangles that comprised the first iteration is removed. This results in the formation of nine metallized triangles. Subsequent iterations are created by repeatedly deleting the mid-point triangle metallization from the metallized triangles that were created by the iteration that came before it.

2.3 Feeding Method

The Feeding for the Sierpinski bow-tie antenna takes place at the location in the middle of its two triangular arms respectively. It is necessary to make use of a balun in order to feed the Sierpinski bow-tie antenna, which is a fully balanced design. This is because the antenna must be supplied by a coaxial or other unbalanced transmission line. When it comes to pattern performance, the performance of the balun has a considerable impact. It is common practice to design the balun so that it can also provide impedance matching. Figure 1(a), 1(b), 1(c) and 1(d) shows the physical dimensions with different views. All the dimensions shown are in millimeters.
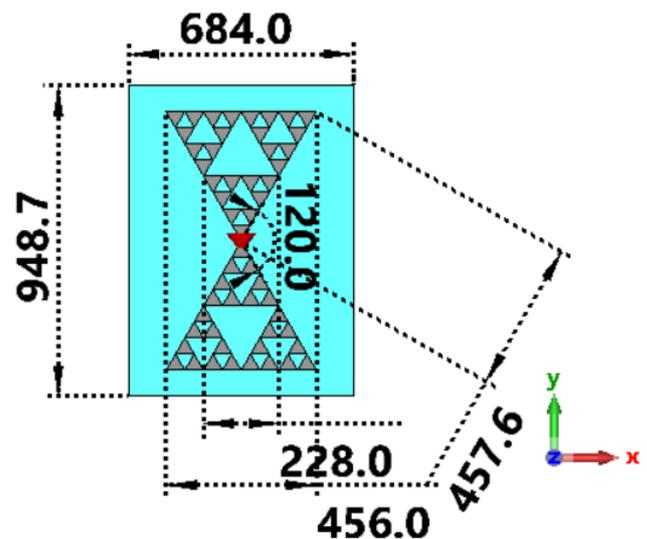

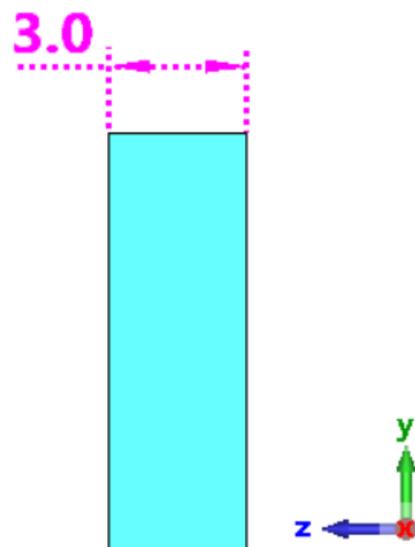**Figure 1(a): Antenna with slotted patch front view (in mm)**

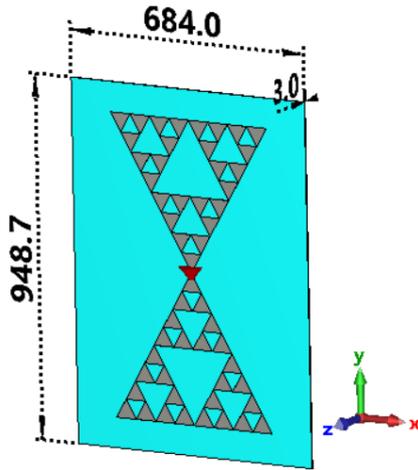**Figure 1(b): Slotted patch antenna side view (in cm)**
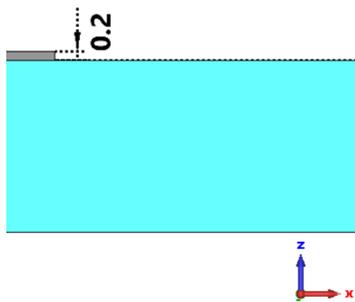

Figure 1 (c): Front View

Figure 1(d): Side view of Slotted Patch antenna in CST (in cm)

2.4 Method of Operation

The self-similarity inherent in an ideal Sierpinski gasket underpins the multi-band performance of this antenna. The image below illustrates this by scaling subsections of the larger gasket to uniform dimensions. The Sierpinski bow-tie exhibits two distinct operational modes. The lowest operational frequency is dictated by the overall length of the antenna; functioning in this low band exhibits characteristics akin to those of a conventional bow-tie antenna. The second lowest operational band denotes the initial fractal band, succeeded by N-1 log-spaced fractal bands for an N-iteration antenna. For instance, if the initial fractal band is at 1 GHz, subsequent fractal bands will be approximately centered. Deviations from the ideal fractally spaced operational bands arise from two types of truncation [12]the first fractal band is impacted by the finite size truncation of the entire antenna, while the Nth band is influenced by the truncation of the fractal geometry. The presence of a dielectric substrate leads to deviations due to variations in electrical thickness across different frequency bands. Experimental findings by [12]. indicate that within each fractal band, most of the energy is concentrated in a circle centered around the feed, with a diameter of approximately 0.75 wavelengths at frequencies of 2, 4, 8, and 16 GHz. The performance of a specific fractal band is minimally affected by the small holes created by subsequent higher fractal iterations, as these holes are electrically small relative to the operational frequency of the lower fractal band.

III. RESULTS AND DISCUSSIONS

A Flexible Sierpinski Bow-tie antenna is being demonstrated here as the antenna that is being displayed. The reflection coefficients of the antenna are depicted in Figure 2 (a), the impedance with real and imaginary with reference to frequency is depicted in Figure 2 (b), and the voltage standing wave ratio at 406 MHz represents 1.5 value at 406 MHz, respectively. All these figures are given in Figure 2. The findings of the inquiry into the fundamental parameter of the antenna are depicted in figures such as this one. It is evident from the graphic that the frequency at which antennas exhibit resonance is 406 MHz. This is the frequency at which resonance occurs. Taking into consideration a bandwidth of 65.53 MHz and a level of -10dB, this is equivalent to 15.90%. After conducting additional research, it was found that the antenna possesses impedance matching that is ideal for the frequency that is intended to be utilized to be utilized.

It is dependent on the number of fractal iterations that are incorporated into the geometry as to whether the Sierpinski bow-tie exhibits suitable impedance behavior in several log-spaced bands. On the other hand, the S_{11} minimum, which has the lowest frequency, is not a fractal band and possesses different performance characteristics. In a perfect world, the fractal bands would be separated in frequency by a factor of two; however, truncation and substrate effects could induce a divergence from this spacing. The use of substrates that are both thicker and have a higher permittivity result in a decrease in the performance of S_{11}. However, substrates that are thicker and have a higher permittivity give rise to the possibility of a minor reduction in the size of the antenna. This is accomplished by reducing the frequency of the initial fractal iteration and the distance between bands.
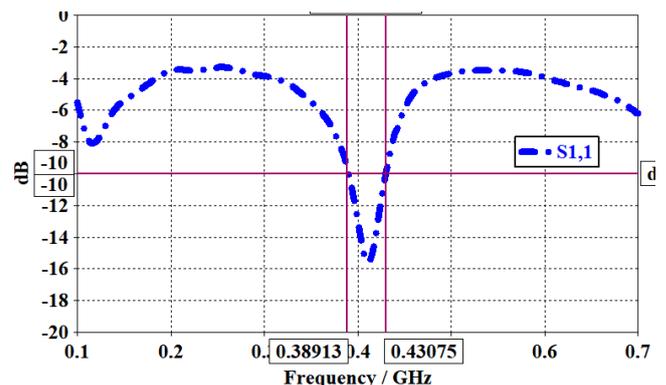
Figure 2(a): Reflection coefficient slotted patch antenna with a -10 dB performance
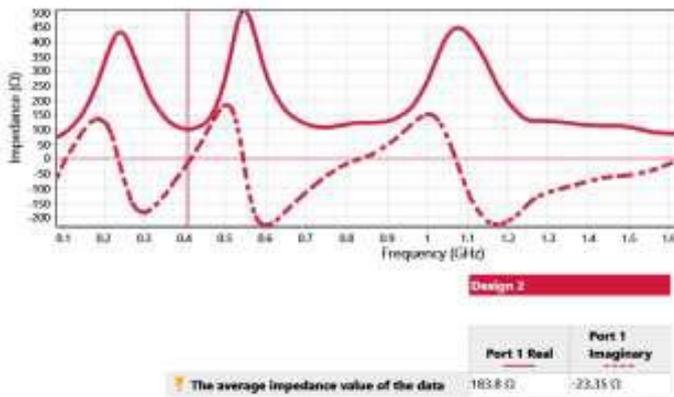

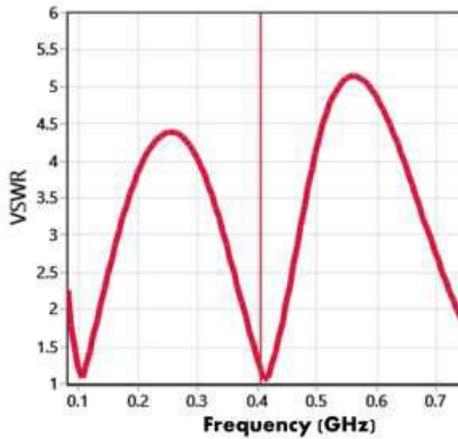**Figure 2(b): Impedance of the antenna with respect to frequency**

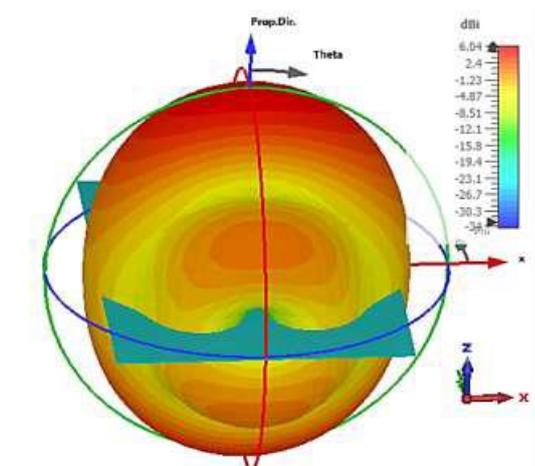**Figure 2(c): Voltage standing wave ratio at 406 MHz**

Figure 3(a): 3D radiation pattern with slotted patch antenna in middle

It has been demonstrated that the antenna has attained gain 3D radiation patterns, which can be seen in Figure 3(a). Because the antenna will be positioned or placed on the beacon, and it will be facing upwards toward the sky, this attribute is extremely significant because the antenna will be placed on the beacon. The maximum gain of the antenna, as measured by the IEEE, can be seen to be in the z-direction, and it is nearly 8dBi. This is easy to see and confirm. Therefore, if the antenna possesses a null at 0 degrees or in the z-direction. If this is the situation, the antenna will be unable to transmit a signal to the satellite on its own.

Theta / Degree vs. dBi

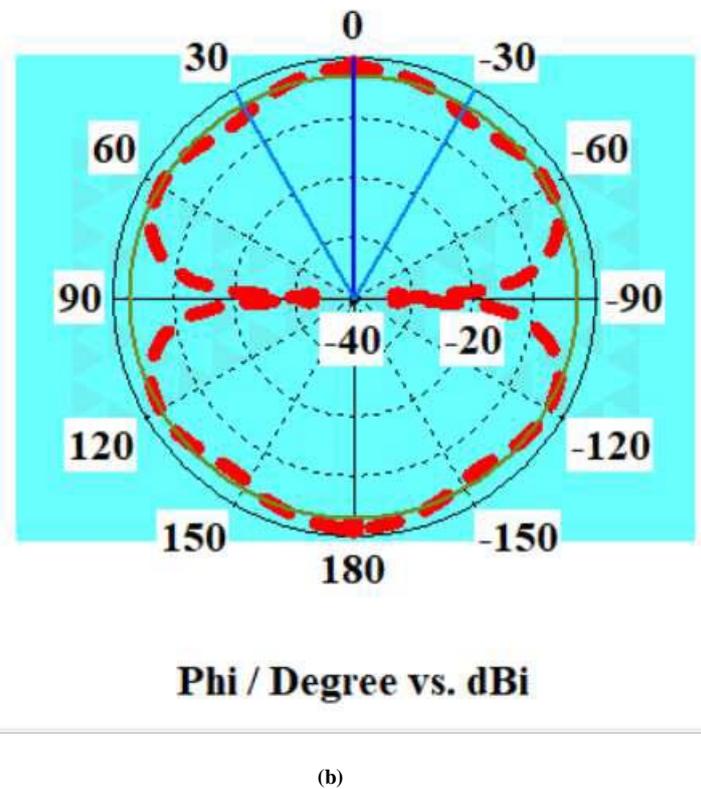**(a)**

Phi / Degree vs. dBi

(b)
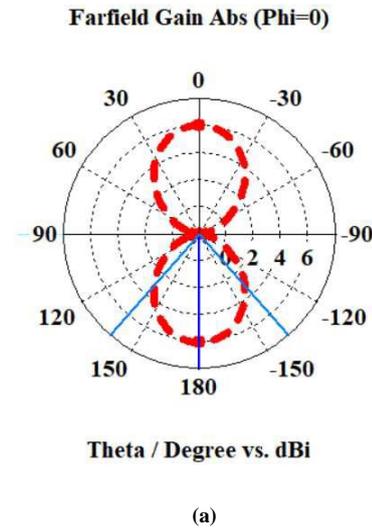
Figure 4: Simulations of Planar Multislot Antenna with Backplane radiation in free space: (a) E_φ ($\varphi = 0^0$), and (b) E_θ ($\theta = 90^0$)

The Fig. 4 (a), and Fig. 4 (b) presents the magnitude of gain in form of radiation patterns for $\varphi = 0^0$ and $\theta = 90^0$. It can be observed that the antenna does not have nulls at 0^0 when $E\varphi$ ($\varphi = 0^0$), and (b) E_θ ($\theta = 90^0$).

IV. CONCLUSION

The main emphasis of the continuous studies is the construction of a unique and flexible COSPAS-SARSAT beacon antenna. This research is under progress right now. Designed particularly for use in the Mission Control Centers of COSPAS-SARSAT, the system runs at a frequency of 406 MHz. Development of this was driven mostly by this. The antenna that has been shown here can so effectively fulfill the two most important goals via the following ways: The first function serves mostly to increase gain at an angle of 0 degrees, which is practically 6dBi. Conversely, the main goal of the second function is to maximize impedance matching at frequency of 406 MHz. The two functions under discussion have a basic incompatible nature. Regarding the overall architectural design of the structure, the ShieldIt Super conducting element is used and the PDMS is applied for the substrate. The basis used to design the whole structure is one that makes creating completely flexible one hundred percent possible. The results of the experiment revealed that the Flexible Sierpinski Bow-tie antenna, running in planar configurations, had an estimated fractional bandwidth of 65.53 MHz, -10dB. This was the outcome when the antenna was placed through circumstances deemed normal.

REFERENCES

[1] S. M. Catalogue and U. States, "COSPAS-SARSAT," pp. 1–85, 2012.

[2] H. Mirza, P. J. Soh, R. A. Sheikh, A. A. Al-Hadi, T. M. Hossain, and S. Yan, "A Flexible Wearable Linear-to-Circular Polarizer for GNSS Application," *ICEICT 2020 - IEEE 3rd Int. Conf. Electron. Inf. Commun. Technol.*, pp. 337–340, 2020.

[3] H. Mirza *et al.*, "Swastika-Shaped Flexible Linear to Circular Polarizer using Textiles," vol. 100, no. 1, pp. 2–4.

[4] G. Kumar, V. K. Singh, and M. B. Mahajan, "Broadband blade antenna operating in UHF band for ELT application," *2nd International Conference on Wireless, Antenna and Microwave Symposium, WAMS 2023*. 2023.

[5] J. V King, "Overview of the Cospas-Sarsat Satellite System for Search and Rescue."

[6] E. Faridah *et al.*, "A Wearable Textile Dipole for Search and Rescue Application," vol. 1, pp. 1–4, 2016.

[7] A. A. Corner, "Body-Worn Antennas Making a Splash : Lifejacket-Integrated Antennas for Global Search and Rescue Satellite System," vol. 55, no. 2, 2013.

[8] A. A. Serra, P. Nepa, and G. Manara, "A Wearable Two-Antenna System on a Life Jacket for Cospas-Sarsat Personal Locator Beacons," vol. 60, no. 2, pp. 1035–1042, 2012.

[9] H. Mirza *et al.*, "Deployable Linear-to-Circular Polarizer Using PDMS Based on Unloaded and Loaded Circular FSS Arrays for Pico-Satellites," *IEEE Access*, vol. 7, pp. 2034–2041, 2019.

[10] T. Hossain *et al.*, "Broadband Single-Layered , Single-Sided Flexible Linear-to-Circular Polarizer Using Square Loop Array for S-Band Pico-Satellites," *IEEE Access*, vol. 7, pp. 149262–149272, 2019.

[11] H. Mirza *et al.*, "A crossed dodecagonal deployable polarizer on textile and polydimethylsiloxane (PDMS) substrates," *Appl. Phys. A Mater. Sci. Process.*, vol. 124, no. 2, p. 178, 2018.

[12] C. Puente-Baliarda, J. Romeu, R. Pous, and A. Cardama, "On the behavior of the sierpinski multiband fractal antenna," *IEEE Trans. Antennas Propag.*, vol. 46, no. 4, pp. 517–524, 1998.

****